Capacitance Extraction for Microstrip Lines Using Conformal Technique Based on Finite-Difference Method

Yaxiu Sun and Xiaomeng Wang

College of Information and Communication Engineering
Harbin Engineering University, Harbin, 150001, China
sunyaxiu@hrbeu.edu.cn, wangxiaomeng@hrbeu.edu.cn

Abstract ─ In this paper, a novel method using conformal technique of finite-difference method (FDM) is proposed to capacitance extraction of microstrip lines. Instead of deriving the average dielectric constant ε, this method uses electric field numerical weights to process the inhomogeneous cells, and takes the discontinuous effects of both inhomogeneous Ampere cell and Faraday cell into account. Besides, a new boundary condition is proposed, where the cells obeying exponential distribution are added at boundary. The new method shows good agreement with the measurement and traditional methods.

Index Terms ─ Capacitance extraction, conformal technique, finite-difference method (FDM).

I. INTRODUCTION

Finte-difference method (FDM) has been widely used to solve variable electromagnetic problems, especially the extraction of distributed parameters [1-3]. When solving the capacitance parameter of microstrip lines, the cells divided from the electromagnetic space can be inhomogeneous, and the dielectric constants in one cell are not unique. Thus, the difference equations cannot be used directly. The general methods solving this problem are equivalent dielectric constant techniques [4-5]. They derive the average dielectric constants according to the relationships of cell loop's volume, area and length, but have neglected the inhomogeneous Faraday and Ampere cells. So a new conformal technique is proposed in this paper, which uses the electric field numerical weights to process inhomogeneous cells, and takes discontinuous effects of Ampere and Faraday cells into account.

Besides, when FDM is used to solve the open structures, boundary conditions are required to terminate the calculation space. Generally, there are two kinds of boundary conditions. One is absorbing boundary condition (ABC) according to the traveling wave equation [6], [7]. The other is perfectly matched layer (PML) based on the absorbing media [8]. ABC requires much less computation and memory than PML, but it may cause higher reflection and larger error. Hence, a new boundary condition is proposed, which cells obeying exponential distribution are added at the boundary. Finally, the proposed conformal technique and new boundary condition are verified by calculation.

II. FORMULATION

A. The iteration equation of FDM

The Gauss law can be represented as:

$$q = \oiint_s \boldsymbol{D} \cdot d\boldsymbol{s}\ , \tag{1}$$

where q is the total electric charge on the surface of the conductor, and $\boldsymbol{D}$ is the electric displacement vector which can be represented as $\boldsymbol{D} = \varepsilon \boldsymbol{E}$. Electric field intensity $\boldsymbol{E}$ can be represented by potential Φ as $\boldsymbol{E} = -\nabla\Phi$. The capacitance solving model is a dual regional structure whose dielectric constants are ε_1 and ε_2 . So the spatial difference equations of $\boldsymbol{E} = -\nabla\Phi$ in these two regions can be described:

$$E_x[(i+\frac{1}{2})\Delta x, j\Delta y] = -\frac{\Phi[(i+1)\Delta x, j\Delta y] - \Phi(i\Delta x, j\Delta y)}{\Delta x}, \tag{2}$$

$$E_y[i\Delta x, (j+\frac{1}{2})\Delta y] = -\frac{\Phi[i\Delta x, (j+1)\Delta y] - \Phi(i\Delta x, j\Delta y)}{\Delta y}, \tag{3}$$

where i and j are any positive integers, Δx and Δy are the step size in x and y direction. So the divergence of electric displacement vector can be derived as:

$$\begin{aligned} &\nabla \cdot \boldsymbol{D}(i\Delta x, j\Delta y) \\ &= -\varepsilon_1 \frac{\Phi[(i+1)\Delta x, j\Delta y] + \Phi[(i-1)\Delta x, j\Delta y] - 2\Phi(i\Delta x, j\Delta y)}{(\Delta x)^2} \cdot \\ &-\varepsilon_2 \frac{\Phi[i\Delta x, (j-1)\Delta y] - 2\Phi[i\Delta x, j\Delta y] + \Phi[i\Delta x, (j+1)\Delta y]}{(\Delta y)^2} \end{aligned} \tag{4}$$

If $\varepsilon_1 = \varepsilon_2$ and $\Delta x = \Delta y$, according to Laplace equation: $\nabla \cdot \boldsymbol{D} = 0$, (4) can be simplified as follows:

$$\begin{aligned} \Phi(i\Delta x, j\Delta y) = \frac{1}{4}\{&\Phi[i\Delta x, (j+1)\Delta y] + \Phi[i\Delta x, (j-1)\Delta y] \\ &+ \Phi[(i+1)\Delta x, j\Delta y] + \Phi[(i-1)\Delta x, j\Delta y]\} \end{aligned}. \tag{5}$$

Equation (1) can be finally updated as:

$$q = -\varepsilon \sum_{i=1}^{\infty}\sum_{j=1}^{\infty} \Phi(i\Delta x, j\Delta y)\ . \tag{6}$$

Submitted On: September 12, 2016
Accepted On: October 18, 2016

Equation (6) is the finite difference iteration equation to solve the capacitance, and the value of per unit length capacitance can be obtained from $C = q/V$.

B. The conformal technology based on FDM

Figure 1 shows the microstrip line model we analysis in this paper. Figure 1 (a) is the discrete grid model. Figure 1 (b) show the structure of microstrip line in Fig. 1 (a). All the simulation calculations in this paper are conducted on the basis of the model of Fig. 1 (b). As shown in Fig. 1 (a), each grid represents a cell. We can see that the dielectric constants of cells at the boundary between two regions cannot be unique. When using the new conformal technology to solve the inhomogeneous cells here, the process is divided into two parts: Faraday cell and Ampere cell.

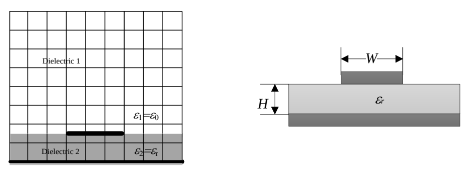

(a) (b)

Fig. 1. (a) The discrete grid model of microstrip line, and (b) structure of microstrip line with *W*/*H*=3, $\varepsilon_r = 4.4$.

As shown in Fig. 2, Faraday cell is divided into two regions with different dielectric constants ε_1 and ε_2 . Δx is divided into two parts: Δx_1 and Δx_2 . The electric field strengths of *x* and *y* direction are also divided into two parts: E_{x1} and E_{x2}, E_{y1} and E_{y2}. θ is the angle between *x* direction and interface.

The spatial derivative of Faraday's law can be written as:

$$\begin{aligned} &E_x^n(i+\frac{1}{2}, j)\Delta x - E_x^n(i+\frac{1}{2}, j+1)\Delta x + E_y^n(i, j+\frac{1}{2})\Delta y - E_y^n(i+1, j+\frac{1}{2})\Delta y \\ &= \mu \frac{1}{\Delta t}[H_z^{n+\frac{1}{2}}(i+\frac{1}{2}, j+1) - H_z^{n+\frac{1}{2}}(i+\frac{1}{2}, j+\frac{1}{2})]\Delta x \Delta y \end{aligned} . \tag{7}$$

According to electric field boundary conditions in perfect dielectric, the weights of dielectric 1 and dielectric 2 are defined as 1 and $\varepsilon_1/\varepsilon_2$ respectively. As shown in Fig. 3, E_{x1} and E_{x2} are discontinuous. Then electric field components can be weighted and the relationship after removing weights are:

$$\begin{cases} E_{x2} = E_{2N}\boldsymbol{e}_n + E_{2T}\boldsymbol{e}_t \\ E'_{2N} = \varepsilon_2 E_{2N}/\varepsilon_1 \\ E'_{2T} = E_{2T} \\ E'_{x2} = E'_{2N}\boldsymbol{e}_n + E'_{2T}\boldsymbol{e}_t \end{cases} , \tag{8}$$

where E'_{x2}, E'_{2N} and E'_{2T} are the weighted components. $\boldsymbol{e}_n$ and $\boldsymbol{e}_t$ are unit vectors.

To ensure the integration value unchanged, the weights of electric field components are taken into integral paths and the final update relationships are:

$$\begin{cases} \Delta N_2 = \Delta x_2 \sin\theta \\ \Delta T_2 = \Delta x_2 \cos\theta \\ \dfrac{\Delta N'_2}{\Delta N_2} = (\dfrac{E'_{2N}}{E_{2N}})^{-1} = \dfrac{\varepsilon_1}{\varepsilon_2} , \\ \dfrac{\Delta T'_2}{\Delta T_2} = (\dfrac{E'_{2T}}{E_{2T}})^{-1} \\ \Delta x'_2 = \sqrt{\Delta T'^2_2 + \Delta N'^2_2} \end{cases} \tag{9}$$

where ΔN_2 and ΔT_2 are the normal component and tangential component after orthogonal decomposition of Δx_2 , $\Delta N'_2$ and $\Delta T'_2$ are the component values of ΔN_2 and ΔT_2 after expanding or reducing. $\Delta x'_2$ is the total length after adjusting the path of field component. So the modified total length of the integral path can be obtained from (9):

$$\Delta x' = \Delta x_1 + \Delta x'_2 = \Delta x_1 + \Delta x_2 \sqrt{\cos^2\theta + \sin^2(\theta \frac{\varepsilon_1^2}{\varepsilon_2^2})} . \tag{10}$$

So we use $\Delta x'$ instead of Δx to calculate (7).

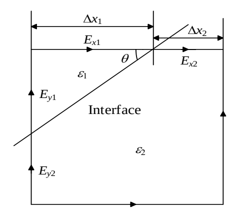

Fig. 2. The inhomogeneous Faraday cell model.

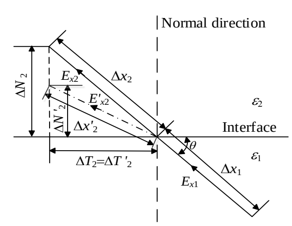

Fig. 3. The conformal process for Faraday loop path.

The conformal process of Ampere cell is same to the Faraday cell, and the Ampere cell model is shown in Fig. 4. The spatial derivative of Ampere's law can be written as:

$$H_z^{n-\frac{1}{2}}(i+\frac{1}{2}, j+\frac{1}{2}) - H_z^{n-\frac{1}{2}}(i+\frac{1}{2}, j-\frac{1}{2}) = \Delta y (\frac{\partial D_x}{\partial t})^n_{(i+1/2, j)} ,\tag{11}$$

Δy is the total length of Ampere loop integral path.

According to electric displacement vectors boundary conditions in perfect dielectric, the weights of two kinds of media can be defined as 1 and $\varepsilon_2/\varepsilon_1$. The positional relationships are shown in Fig. 5. So the relationship between the components after removing the weights can be written as:

$$\begin{cases} D'_{2N} = D_{2N} \\ D'_{2T} = D_{2T}\,\varepsilon_1/\varepsilon_2 \end{cases}, \tag{12}$$

where D'_{2N} and D'_{2T} are the weighted components. Then taking the weights into the integral path:

$$\begin{cases} \Delta T_2 = \Delta y_2 \cos\varphi \\ \Delta N_2 = \Delta y_2 \sin\varphi \\ \dfrac{\Delta N'_2}{\Delta N_2} = \left(\dfrac{D'_{2T}}{D_{2T}}\right)^{-1} = \dfrac{\varepsilon_2}{\varepsilon_1}\,, \\ \dfrac{\Delta T'_2}{\Delta T_2} = \left(\dfrac{D'_{2N}}{D_{2N}}\right)^{-1} \\ \Delta y'_2 = \sqrt{\Delta N'^2_2 + \Delta T'^2_2} \end{cases} \tag{13}$$

where ΔN_2 and ΔT_2 are the initial length of normal and tangential component, which are obtained from orthogonal decomposition Δy_2, $\Delta y'_2$. $\Delta N'_2$ and $\Delta T'_2$ are the length after adjusting the path of field component. So the modified total length of the integral path is:

$$\Delta y' = \Delta y_1 + \Delta y'_2 = \Delta y_1 + \Delta y_2\sqrt{\cos^2\phi + \sin^2\phi\,\frac{\varepsilon_1^2}{\varepsilon_2^2}}\,. \tag{14}$$

So we use $\Delta y'$ instead of Δy to calculate (11).

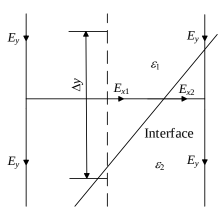

Fig. 4. The inhomogeneous Ampere cell model.

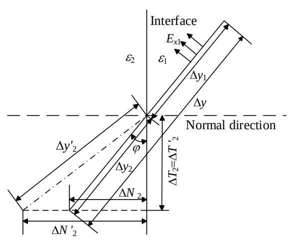

Fig. 5. The conformal process for Ampere loop path.

After above process, ε_2 and ε_1 has been converted as ε_e. So the relationship between electric field strength and electric displacement can be expressed by $\boldsymbol{D} = \varepsilon_e \boldsymbol{E}$.

C. A new boundary condition

A new boundary condition is proposed in the paper, which cells obeying exponential distribution are added at the boundary. Taking x direction for example, the electric field distribution obeys e^{-kx}, where k is a positive number. The outermost cells are considered infinitely long. When x tends to infinity, e^{-kx} is close to zero. So the outermost cells are described and the potentials are zero at infinity points.

III. NUMERICAL RESULTS

To verify the validity of new boundary condition, we use the mesh $\Delta x = \Delta y = 10^{-3}$m to calculate the region where the coordinate is $x \in [-39\Delta x, 39\Delta y]$ and $y \in [-39\Delta x, 39\Delta y]$. The potential at infinity is set at 0. We add the conductors with +10V at $(-20\Delta x, -20\Delta y)$ and -10V at $(20\Delta x, 20\Delta y)$ respectively.

Now the electric field distributions using different boundary conditions are shown in Fig. 6 and Fig. 7. One is the traditional boundary condition which is similar to a rectangle shield and the potential is $\Phi = 0$. The other is the new boundary condition in this paper. The electric field strength shown in Fig. 6 attenuates slowly in the diagonal direction. Whereas the electric field strength shown in Fig. 7 is closer to the potential distribution model with the same amount unlike charges. So the new boundary condition proposed in this paper is more applicable to solve the capacitance.

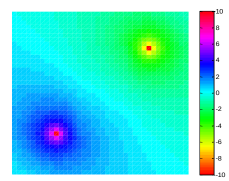

Fig. 6. The electric field distribution under traditional boundary condition.

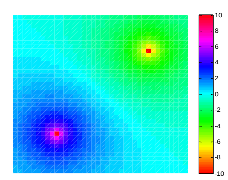

Fig. 7. The electric field distribution under new boundary condition.

Now the new method using conformal technique and new boundary condition has been applied to calculate the capacitance of microstrip line in Fig. 1. There are 79×79 grids in simulation area, and we use the mesh $\Delta x = \Delta y = 10^{-3}$m to calculate the region where the coordinate is $x \in [-39\Delta x, 39\Delta y]$ and $y \in [-39\Delta x, 39\Delta y]$. The potential at infinity is set at 0. The potential of microstrip line at $[-39\Delta x \le x \le 39\Delta x, -39\Delta y \le y \le -38\Delta y]$ is +10V, and the potential of microstrip line at $[-6\Delta x \le x \le 6\Delta x, -35\Delta y \le y \le -34\Delta y]$ is -10V. The dielectric constant is $\varepsilon_r = 4.4$, which is distributed in the area of $[-39\Delta x \le x \le 39\Delta x, -38\Delta y \le y \le -35\Delta y]$.

Figure 8 and Fig. 9 show the potential distributions of Fig. 1 under the new boundary. Whereas the Fig. 9 has used the conformal technique and Fig. 8 has not. The scattered field at the cross media shown in Fig. 9 is more obvious than in Fig. 8. Moreover, the per unit length capacitance obtained from Fig. 8 is 101.47pF/m, and the value obtained from Fig. 9 is 97.759pF/m. Furthermore, the per unit length capacitance has been measured by the static field capacitance measurement method. It uses galvanometer measured the charge of microstrip line in case of a given voltage. Then the per unit length capacitance can be obtained and the value is 97.761pF/m. So the value of capacitance is closer to the measurement when using new conformal technology.

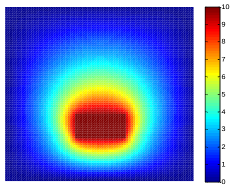

Fig. 8. The potential distribution without using conformal technique.

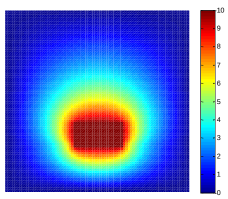

Fig. 9. The potential distribution using conformal technology.

Besides, to verify the accuracy of new method further, the average dielectric constant method has been used to calculate the capacitance of the microstip line model in Fig. 1 (b), and the discrete grid model is shown in Fig. 10. The potential distribution using the average dielectric constant method is shown in Fig. 11, and the per unit length capacitance is 96.87pF/m. The comparative result shows that the capacitance calculated by the new method is more approximated to the measurement than the average dielectric constant method. It shows that the new method has higher precision than the average dielectric constant method.

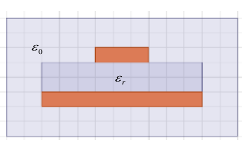

Fig. 10. The microstrip line model using average dielectric constant method.

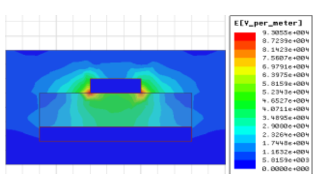

Fig. 11. The potential distribution of Fig. 10 model.

IV. CONCLUSION

A new method based on FDM has been proposed for capacitance extraction of microstrip line using conformal technique. The results show that the capacitance solved by the proposed method is close to the measurement and more accurate than traditional one. Besides, the new method can be applied to various positional relationships between dielectric interface and electric field directions. It also has a significance to the analysis and design of high speed PCB.

ACKNOWLEDGMENT

This project was supported by the National Natural Science Foundation of China (Grant No. 51209055), the China Postdoctoral Special Foundation (Grant No. 2015T80324), and the Natural Science Foundation of Heilongjiang, China (Grant No. F2015028).

REFERENCES

[1] Y. Liu, K. Lan, and K. Mei, "Capacitance extraction for electro static multiconductor problems by on-surface MEI," *IEEE Trans. Advanc. Packag.*, vol. 23, no. 3, pp. 489-494, 2000.

[2] J. Wang, W. Y. Yin, and Q. H, Liu, "FDTD (2, 4)-compatible conformal technique for treatment of dielectric surfaces," *Electronics Lett.*, vol. 45, no. 3, pp. 146-147, Jan. 29, 2009.

[3] J. Wang, W. Y. Yin, and Y. S. Xia, "A novel conformal surface current technique for large problems based on high-performance parallel FDTD method," *IEEE Antennas and Wireless Propag. Lett.*, vol. 12, pp. 11-14, 2013.

[4] L. Liou, Y. Mah, and A. Ferendeci, "Equivalent circuit parameter extraction of microstrip coupling lines using FDTD method," *IEEE Int. Symp. Antennas Propag.*, vol. 3, pp. 2488-1491, 2000.

[5] W. Yu and R. Mittra, "A conformal finite difference time domain technique for modeling curved dielectric surfaces," *IEEE Microw. Wireless Comp. Lett.*, vol. 11, no. 1, pp. 25-27, Jan. 2001.

[6] J. Zhou and J. Zhao, "Efficient high-order absorbing boundary conditions for the ADI-FDTD method," *IEEE Microw. Wireless Comp. Lett.*, vol. 19, no. 1, pp. 25-27, Jan. 2009.

[7] H. Shao, W. Hong, and Y. Zhou, "Generalized Z-domain absorbing boundary conditions for the analysis of electromagnetic problems with finite-difference time-domain method," *IEEE Trans. Microw. Theory Tech.*, vol. 51, pp. 82-90, 2003.

[8] S. Wang and F. L. Teixeira, "An efficient PML implementation for the ADI-FDTD method," *IEEE Mirow. Wireless Compon. Lett.*, vol. 13, no. 2, pp. 72-74, Feb. 2003.